

UC Berkeley

UC Berkeley Previously Published Works

Title

Effect of Molecular Weight and Salt Concentration on Ion Transport and the Transference Number in Polymer Electrolytes

Permalink

<https://escholarship.org/uc/item/8wk9n75f>

Journal

Macromolecules, 48(21)

ISSN

0024-9297

Authors

Timachova, Ksenia
Watanabe, Hiroshi
Balsara, Nitash P

Publication Date

2015-11-10

DOI

10.1021/acs.macromol.5b01724

Peer reviewed

Effect of Molecular Weight and Salt Concentration on Ion Transport and the Transference Number in Polymer Electrolytes

Ksenia Timachova, Hiroshi Watanabe,[†] and Nitash P. Balsara^{*,‡}

Department of Chemical and Biomolecular Engineering, University of California Berkeley, Berkeley, California 94702, United States

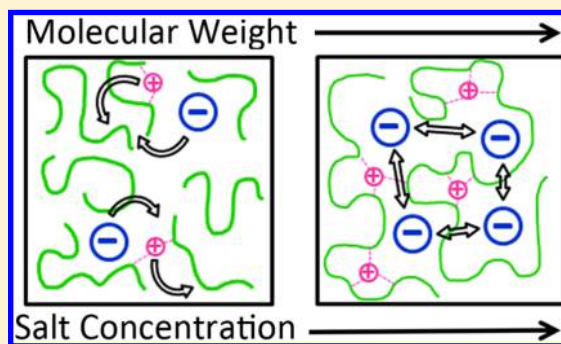
[†]Institute for Chemical Research, Kyoto University, Uji, Kyoto 611-0011, Japan

[‡]Department of Chemical and Biomolecular Engineering, University of California Berkeley, Berkeley, California 94702, United States
Materials Science Division, Lawrence Berkeley National Laboratory, Berkeley, California 94720, United States

Energy Storage and Distributed Resources Division, Lawrence Berkeley National Laboratory, Berkeley, California 94720, United States

S Supporting Information

ABSTRACT: Transport of ions in polymer electrolytes is of significant practical interest, however, differences in the transport of anions and cations have not been comprehensively addressed. We present measurements of the electrochemical transport properties of lithium bis(trifluoromethanesulfonyl)imide (LiTFSI) in poly(ethylene oxide) (PEO) over a wide range of PEO molecular weights and salt concentrations. Individual self-diffusion coefficients of the Li^+ and TFSI^- ions, D_+ and D_- , were measured using pulsed-field gradient nuclear magnetic resonance both in the dilute limit and at high salt concentrations. Conductivities calculated from the measured D_+ and D_- values based on the Nernst–Einstein equation were in agreement with experimental measurements reported in the literature, indicating that the salt is fully dissociated in these PEO/LiTFSI mixtures. This enables determination of the molecular weight dependence of the cation transference number in both dilute and concentrated solutions. We introduce a new parameter, s , the number of lithium ions per polymer chain, that allows us to account for both the effect of salt concentration and molecular weight on cation and anion diffusion. Expressing cation and anion diffusion coefficients as functions of s results in a collapse of D_+ and D_- onto a single master curve.



INTRODUCTION

Polymer electrolytes are of great interest due to their potential use in high specific energy lithium batteries.¹ These materials are generally mixtures containing dissociated ions in a polymer matrix. Poly(ethylene oxide) (PEO) is the most widely studied polymer electrolyte due to its ability to solvate and conduct lithium ions^{2,3} and lithium bis(trifluoromethanesulfonyl)imide (LiTFSI) is a commonly used salt in PEO-based electrolytes.⁴

The performance of binary electrolytes such as PEO/LiTFSI in batteries is governed by three transport coefficients. Newman and co-workers have pioneered the use of ionic conductivity σ , the mutual diffusion coefficient of the salt D_m , and the cation transference number t_+ to predict battery performance.⁵ The parameter t_+ provides a measure of the fraction of ionic current carried by the cation, while D_m quantifies the transport of salt molecules due to gradients in chemical potential in the absence of electric fields. They have also prescribed methods for measuring these three quantities. The salt diffusion coefficient is obtained from restricted diffusion measurements on symmetric lithium–polymer–lithium cells.⁶ Measurement of the transference number required two additional experiments: current-interrupt experiments and open circuit potential

measurements of concentration cells, wherein polymer electrolytes of different concentrations are brought in contact with each other.⁷ The attractiveness of this approach is that battery performance can be predicted using σ , D_m , and t_+ without any knowledge of the extent of dissociation of the salt molecules. The effect of salt dissociation is completely captured by the measured values of σ , D_m , and t_+ .

Several alternative methods for measuring transport quantities related to D_m and t_+ have been proposed. There are many reports of transference numbers obtained by potentiostatic polarization of symmetric cells. Doyle and Newman showed that this approach for measuring t_+ can lead to substantial errors.⁸ They studied a 2.8 M solution of NaCF_3SO_3 (sodium triflate) in PEO at 85 °C. While the potentiostatic polarization method gave a t_+ of 0.37, the more rigorous method of Ma et al. gave -4.38 . Another approach is based on pulsed-field gradient nuclear magnetic resonance (PFG–NMR) wherein the self-diffusion of individual species is measured. Battacharja et al.

Received: August 6, 2015

Revised: October 1, 2015

Published: October 19, 2015

used ^7Li and ^{19}F NMR to separately quantify the diffusion of lithium- and fluorine-containing species in PEO/lithium triflate (PEO/LiTf) mixtures as a function of temperature.⁹ Gorecki and Armand have conducted extensive NMR studies of crystallinity and the temperature dependencies of diffusion and relaxation phenomena in PEO electrolytes including PEO/LiTFSI.^{10–12} They found correlation between the motion of lithium ions and the relaxation of protons on the polymer chain, while the anion motion remained independent of the polymer chain.

Using PFG–NMR to predict battery performance, however, requires knowledge of the state of dissociation because the measurement probes all species containing the element of interest.¹³ If LiTFSI is completely dissociated to give Li^+ and TFSI^- then the PFG–NMR experiments quantify the self-diffusion of individual ions. In the dilute limit, measurements of conductivity and the self-diffusion coefficients of the anion and cation, D_+ and D_- , allow us to calculate any transport property. In binary electrolytes,

$$t_+ = \frac{D_+}{D_+ + D_-} \quad (1)$$

$$D_m = \frac{2D_+D_-}{D_+ + D_-} \quad (2)$$

In concentrated solutions, however, the relationships between D_+ , D_- , D_m , and t_+ are not simple due to effects such as nonideal solution behavior and ion clustering.

The effect of chain length on transport of neutral molecules through polymeric materials has been studied extensively.^{14–19} In contrast, relatively few publications have reported measurements of the effect of chain length on ion transport through polymers. Shi and Vincent used electrochemical methods and PFG–NMR to determine the lithium cation diffusion coefficient and steady-state current in PEO/LiTf mixtures as a function of PEO molecular weight, M .²⁰ The conductivity of PEO/LiTFSI mixtures has been measured as a function of M by Teran et al. and Devaux et al.^{21,22} Hayamizu et al. have measured the diffusion coefficients of lithium and TFSI by PFG–NMR as a function of M for oligomeric PEO chains with $M \leq 2.5$ kg/mol.²³ Theoretical studies of the effect of chain length on ion transport in PEO-based electrolytes have also been conducted.^{24–26} A comprehensive study of the effect of polymer molecular weight and salt concentration on cation and anion diffusion and t_+ has not been conducted.

In this work, we use PFG–NMR to study the transport of cations and anions in PEO/LiTFSI mixtures. We present data on the dependence of the cation and anion self-diffusion coefficients, D_+ and D_- , and the cation transference number t_+ on M over the range 0.6–100 kg/mol. Our work suggests that the three transport coefficients, conductivity σ measured by ac impedance, and D_+ and D_- measured by NMR, can be used to fully characterize both dilute and concentrated PEO/LiTFSI mixtures. Our measurements highlight the difference in the coupling of ion transport and polymer segmental motion between cations and anions. In spite of this, we present a framework for collapsing the dependence of D_+ and D_- on salt concentration and molecular weight into a single curve.

EXPERIMENTAL SECTION

Materials. Hydroxyl-terminated PEO samples up to 55 kg/mol were obtained from Polymer Source, 100 kg/mol PEO was obtained from Sigma-Aldrich, and LiTFSI salt was obtained from Novolyte.

PEO molecular weight was varied from 0.6 kg/mol to 100 kg/mol. The characteristics of the polymers used in this study are listed in Table 1. The molecular weight and dispersity were provided by the

Table 1. Properties of Polymers Used in the Study

M (kg/mol) ^a	D^b	[EO]/chain
0.6	1.03	15
1	1.10	23
2	1.10	45
4	1.03	91
10	1.05	230
20	1.10	450
55	1.28	1250
100 ^c	–	2270

^a M = number-averaged molecular weight. ^b D = dispersity. ^c[EO]/chain = number of monomers per chain. ^c M_v reported.

manufacturers. All materials were dried under vacuum at 90 °C for 24 h before use in an air and water-free Argon environment. LiTFSI salt was mixed directly with 0.6 kg/mol PEO and the remaining samples were prepared by mixing PEO and LiTFSI with anhydrous tetrahydrofuran (THF) at 90 °C for 12 h, subsequently allowing the THF to evaporate. Varying salt concentrations were mixed, ranging from $r = 0.01$ to $r = 0.08$, with r defined as the ratio of lithium ions to ethylene oxide (EO) monomer units: $r = [\text{Li}]/[\text{EO}]$. The electrolyte solutions were again dried at under vacuum at 90 °C for 24 h to remove any remaining solvent and placed into NMR tubes. All NMR tubes were sealed with high pressure polyethylene caps before measurement.

Pulsed Field Gradient–NMR (PFG–NMR). NMR measurements were performed on a Bruker Avance 600 MHz instrument fitted with a Z-gradient direct detection broad-band probe and a variable temperature unit maintained at 363 K throughout the experiments. Measurements were performed on the isotopes of ^7Li and ^{19}F to probe the diffusion of lithiated and fluorinated species, respectively. All samples produced single peaks around 233 MHz for lithium and 565 MHz for fluorine corresponding to all lithium- and TFSI-containing ion species, consistent with the measured ions being in the fast exchange limit. The 90° pulse lengths were optimized for each sample to achieve maximum signal amplitude. T1 relaxation times were independently measured for each sample nuclei using inversion–recovery (180– τ –90–acq.) to ensure the choice of an appropriate diffusion time interval Δ . A bipolar pulse longitudinal-eddy-current delay sequence was used to measure the diffusion coefficients D .²⁷ The attenuation of the echo E was fit to,

$$E = e^{-\gamma^2 g^2 \delta^2 D (\Delta - \delta/3 - \tau/2)} \quad (3)$$

where γ is the gyromagnetic ratio, g is the gradient strength, δ is the duration of the gradient pulse, Δ is the interval between gradient pulses, τ is the separation between pulses, and D is the diffusion coefficient. The diffusion time Δ and gradient pulse length δ were independently varied to confirm that they do not affect the measured value of D . Parameters used for acquisition were diffusion intervals $\Delta = 0.4$ – 0.5 s (^7Li) and 0.8 – 1 s (^{19}F), and pulse lengths $\delta = 5$ – 20 ms (^7Li) and 1 – 4 ms (^{19}F). For each diffusion measurement, 32 experiments of varying gradient strength up to 0.5 T/m were performed and the change in amplitude of the attenuated signal was fit to obtain the parameter D . All measured signal attenuations were single exponential decays and the errors in the fits were less than 3% (^{19}F) and 2% (^7Li). Error corresponding to the reproducibility of the data is shown for all samples with two or more independent measurements; the error bars correspond to the range of measured values. Because of the complexity and length of the PFG–NMR measurements at slow diffusion times, not all molecular weights include more than one sample. Single data points are marked with an \times in the figures presented.

RESULTS AND DISCUSSION

The dependence of lithium and TFSI diffusion coefficients, D_{Li} and D_{TFSI} , on salt concentration in a 4 kg/mol PEO at 363 K is shown in Figure 1. As expected, the diffusivity of TFSI is higher

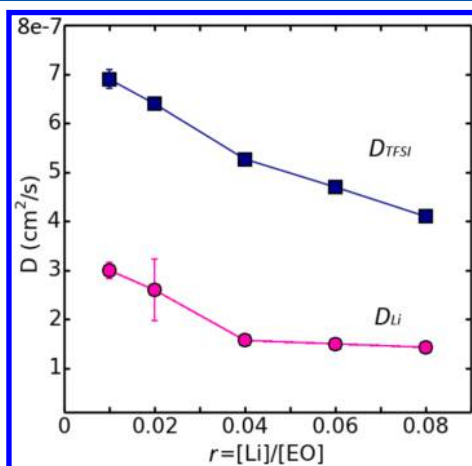


Figure 1. Diffusion coefficients D_{Li} and D_{TFSI} as a function of salt concentration $r = [Li]/[EO]$ in a 4 kg/mol PEO at 363 K. Error bars represent the range of measured values. In most cases, the error is smaller than the marker.

than that of lithium despite the lithium being much smaller. This is due to interactions between Li^+ and ether oxygens in PEO, and the lack of such interaction in the case of TFSI.^{3,28–30} Both diffusion coefficients decrease with increasing salt concentration due to two possible effects: (1) increasing viscosity of PEO/LiTFSI mixtures due to temporary “crosslinks” between polymer chains in the vicinity of the Li^+ ions, (2) ion–ion interactions resulting in the formation of temporary neutral or charged clusters. The measured ionic conductivity of PEO/LiTFSI increases linearly with r when $0 < r < 0.04$ and peaks at $r = 0.085$.⁴ In other words, increasing the charge carriers concentration above $r = 0.085$ reduces overall ion transport. In dilute electrolyte solutions, conductivity increases linearly with charge carrier concentration, therefore, mixtures in the vicinity of $r = 0.085$ are not dilute. In the discussion below, we will examine the effect of molecular weight M on diffusion in two limits, the dilute limit at $r = 0.02$ and the concentrated regime near the maximum of conductivity at $r = 0.08$.

The diffusion of lithium and TFSI species as a function of PEO molecular weight M is shown in Figure 2. The diffusion coefficients D_{Li} and D_{TFSI} decrease with increasing molecular weight. These data are qualitatively consistent with the prevailing theories of ion transport in polymer electrolytes,^{20,24,31,32} which suggest that in the low molecular weight regime, ion hopping due to segmental motion is augmented by diffusion of entire polymer chains with coordinated ions, while, at high molecular weights, chain diffusion slows down, and ion transport is dominated by hopping. There are, however, some differences between the behaviors of D_{Li} and D_{TFSI} at different concentrations shown in Figure 2. At $r = 0.02$, D_{TFSI} approaches a well-defined plateau at $M > 4$ kg/mol, while D_{Li} seems to decrease more slowly, reaching a plateau at $M > 10$ kg/mol. At $r = 0.08$, D_{TFSI} is at a plateau for all values of M , while D_{Li} again decreases continuously with increasing M . The qualitative differences seen in the measurements of D_{Li} and D_{TFSI} at high

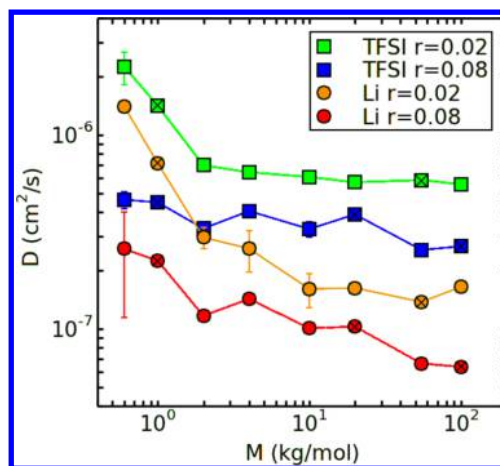


Figure 2. Diffusion coefficients, D , as a function of PEO molecular weight, M , of lithium and TFSI species at salt concentrations of $r = 0.02$ (green, orange) and $r = 0.08$ (blue, red) at 363 K. Measurements with a single data point, present due to the difficulty and length of the PFG–NMR experiment, are marked with an \times . In most cases, the error bars are smaller than the marker.

and low concentrations cannot be readily explained by prevailing theories of ion transport in polymer electrolytes.^{20,25}

In order to probe the state of dissociation in the PEO/LiTFSI mixtures, we used D_{Li} and D_{TFSI} to calculate ionic conductivity using the Nernst–Einstein equation,

$$\sigma = \frac{F^2 c_+}{RT} (D_- + D_+) \quad (4)$$

where T is the temperature, R is the gas constant, F is Faraday’s constant, c_+ is the concentration of dissociated cations [mol/cm^3], and D_+ and D_- are the self-diffusion coefficients of the cation and anion, respectively. It is important to note that eq 4 was developed for dilute solutions where the salt is completely dissociated. Equation 4 assumes that the dominant charge carriers are dissociated ions, therefore, D_+ and D_- could be different from D_{Li} and D_{TFSI} measured by NMR. If our mixtures were to contain clusters of associated ions, then D_{Li} and D_{TFSI} would represent the average diffusion coefficients of all charged and neutral species containing lithium and fluorine, respectively. Conductivity only depends on the transport of charged species.

In Figure 3, the conductivity calculated using eq 4 is plotted as a function of M . In this case, D_{Li} and D_{TFSI} were used for D_+ and D_- , and the total salt concentration was used for c_+ . In Figure 3a, the predictions in the dilute limit, $r = 0.02$, are compared to conductivity values reported in literature; the comparison is limited to two available molecular weights reported by Singh et al. and Lascaud et al.^{4,33} Here we see quantitative agreement between our calculations and experiment. This indicates that all of the salt is dissociated and ion transport is dominated by free cations and anions. We expect eq 4 to hold for dilute PEO/LiTFSI mixtures.

In Figure 3b, we compare calculations based on eq 4 in the concentrated limit, $r = 0.08$, with ionic conductivity measurements reported by Teran et al.²¹ We again see quantitative agreement between our calculations and experiments. This indicates that the total salt concentration is equal to the concentration of dissociated cations c_+ and the self-diffusion coefficients measured in the concentrated regime embody all of the complexities necessary to predict ionic conductivity. We

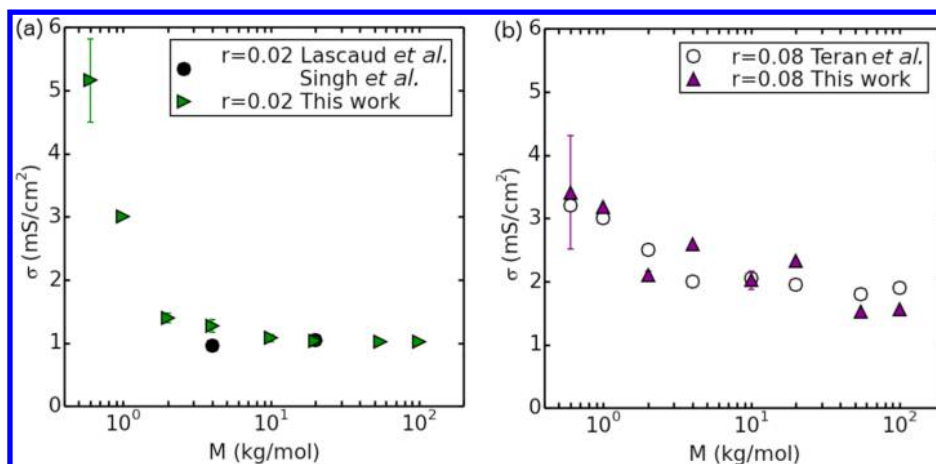


Figure 3. Conductivity calculated from diffusion measurements based on the Nernst–Einstein relation (triangles) and electrochemically measured value of conductivity reported in literature (circles) as a function of PEO molecular weight, M . (a) Comparisons in the dilute limit, $r = 0.02$, with Singh et al. and Lascaud et al.^{4,33} (b) Comparisons in the concentrated regime, $r = 0.08$, with Teran et al.²¹ Error bars represent the range of measured values. In most cases, the error is smaller than the marker.

conclude that $D_+ = D_{Li}$ and $D_- = D_{TFSI}$ in both the dilute and concentrated regimes. We can thus estimate the lithium transference number t_+ according to eq 2 irrespective of the concentration regime.

The lithium transference number t_+ is plotted as a function of M in Figure 4. In both dilute and concentrated regimes, t_+

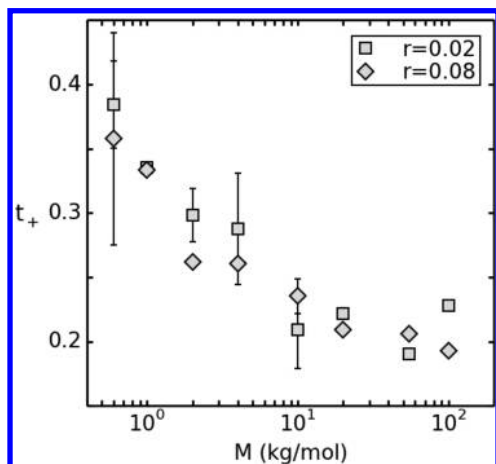


Figure 4. Cation transference number t_+ as a function of PEO molecular weight, M , for salt concentrations $r = 0.02$ and $r = 0.08$ at 363 K. Error bars represent the range of measured values. The error is smaller than the marker where the error bars are not visible.

decreases with increasing M . At low molecular weights, diffusive motion of the polymer contributes more equally to the motion of both ions, and we see a transference number that approaches 0.5. Above 10 kg/mol, ion motion becomes limited to the segmental motion of the polymer chains and t_+ approaches a plateau. It is interesting to note that while D_+ and D_- are sensitive functions of salt concentration (Figure 2), t_+ is not.

We posit that the dependence of D_+ and D_- on salt concentration is related to the strong tendency for lithium ions to coordinate with ether oxygens on either a single chain or on two neighboring chains; both coordination environments are observed in simulations with roughly equal probability.^{28,29} As a result, PEO/LiTFSI electrolytes are comprised of two kinds of chains: chains with a coordinated lithium ions and free PEO

chains. The role of this heterogeneity is elucidated by introducing a parameter s , which we define as the molar ratio of lithium ions to PEO chains, $s = [Li]/\text{chain}$ ($s = r \times N$, where N is the number of ethylene oxide monomers per chain). Not all chains will have coordinated lithium ions when s is much less than one, while when s is much larger than one, one expects most of the chains to be coordinated. In Figure 5, we plot D_+ and D_- as a function of s at four different concentrations: $r = 0.02$ and $r = 0.08$ from this work, and $r = 0.05$ and $r = 0.1$ obtained from Hayamizu et al. and interpolations of data of a 5000 kg/mol PEO from Oradd et al.^{23,34} It is important to note that the PEO chains in this work are hydroxyl terminated while the PEOs in Hayamizu et al. are methyl terminated. It is likely that the small offset in measured diffusivity values in the low molecular weight limit is due to this difference (D_+ and D_- at $r = 0.05$ and $r = 0.1$ from Hayamizu et al. are slightly above the $r = 0.02$ and $r = 0.08$ data from the present work at $M < 1$ kg/mol). Organizing the diffusivities with the parameter s allows us to see that the dependences of D_+ and D_- on M obtained at all salt concentrations are similar.

We fit the data in Figure 5 to power law functions of $\log |D - D_p| = m \log(s) + \log(K)$ where m is the slope, $\log(K)$ is the y -intercept, and D_p is the plateau value at each concentration. An average slope of $m = -1$ and y -intercept of $K = -6.48$ cm²/s was found to reasonably fit the data at all salt concentrations. The dashed lines in Figure 5 are curves of

$$D_i = Ks^{-1} + D_{p,i}, \quad i = +, - \quad (5)$$

where $D_{p,i}$ is the plateau value, shown as a function of r in Figure 6. It is worth noting that $D_{p,i}$ depends on r and i , while the parameter K is independent of r and i . The observation that t_+ vs M is independent of salt concentration in Figure 4 is consistent with the notion that K is independent of r and i ; see eq 1.

In Figure 5a, we show that D_+ at all salt concentrations decreases with increasing s . This reflects an increasing number of coordinated lithium ions per chain that slow down the motion of the ion carrying segments and consequently D_+ . At high values of s , this effect saturates and D_+ approaches a plateau. Similarly, as shown in Figure 5b, D_- decreases with increasing s and reaches a plateau above $s = 10$. Although the anion is not coordinated to PEO, D_- changes with s when $s <$

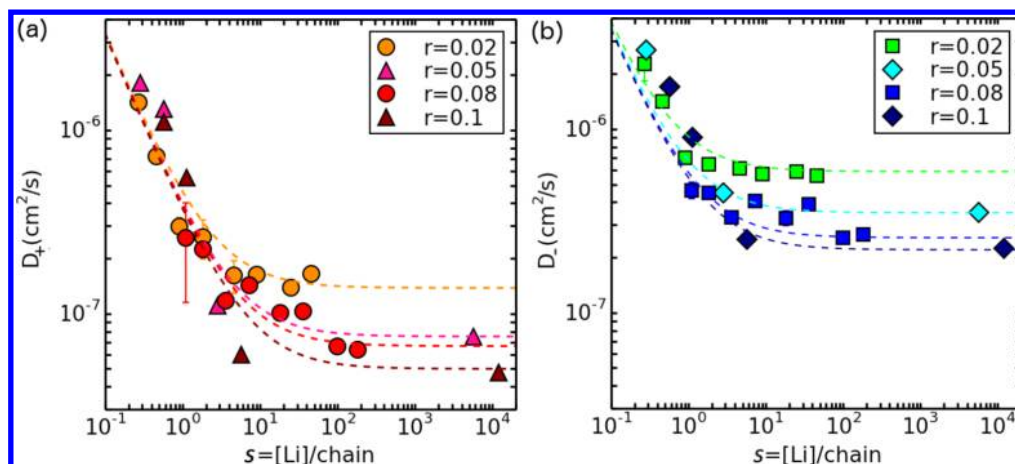


Figure 5. Diffusion coefficients (a) D_+ and (b) D_- as a function of $s = [\text{Li}]/\text{chain}$ at salt concentrations of $r = 0.02$ and $r = 0.08$ from this work, and $r = 0.05$ and $r = 0.1$ taken directly from Hayamizu et al. and interpolated from the data of Oradd et al.^{23,34} Fits of the data (dotted lines) to $D_i = Ks^{-1} + D_{p,i}$ are shown. Error bars are shown only for our data. The error is smaller than the marker where the error bars are not visible.

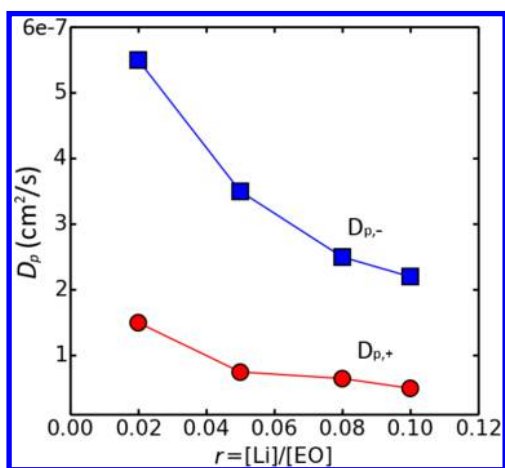


Figure 6. Plateau values D_p of the cation and anion plotted as a function of molar salt concentration r .

10. This behavior is related to the coupling of the anion and cation across distances commensurate with the Bjerrum length, discussed below.

As can be seen in Figure 6, the plateau of $D_{p,-}$ is at significantly higher values than $D_{p,+}$. In the high concentration limit, the motion of the cation and anion are decoupled. The ratio $D_{p,-}/D_{p,+}$ is about 5, reflecting the fact that only the cations are coordinated by the PEO chains. In a given time interval, the anions, on average, diffuse across distances that are a factor of 2.2 ($\sim\sqrt{5}$) larger than that of the lithium ion. Since the ions exist as dissociated pairs, several anions diffuse in and out of the neighborhood of a given cation before the cation hops to a new coordination site. This motion is facilitated by the small distance between dissociated pairs of cations and anions. In the low salt concentration limit, a single parameter K that is independent of the ion species captures the decrease of D_+ and D_- with increasing s . In this limit, the distance between pairs of ions is much greater than the Bjerrum length, l_B ($l_B = 7.5$ nm in PEO, assuming a dielectric constant of 7.5). This precludes independent and rapid diffusion of the more mobile anion between neighboring solvated cations. As a result, the decrease of D_- with increasing s is synchronized with the decrease of D_+ , the coordinated cation.

In Figure 7, the dependence of the diffusion coefficients on r and M is shown on plots of $(D - D_p)$ versus s . Both cation and

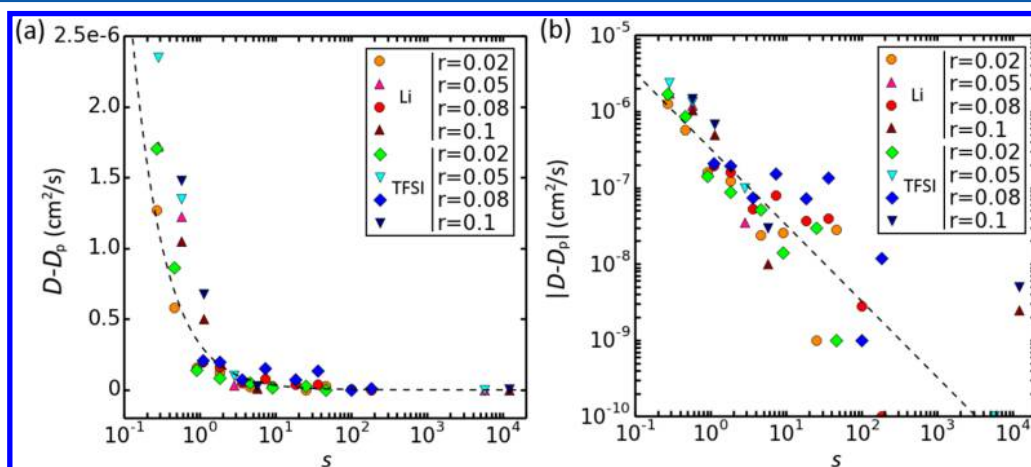


Figure 7. $D - D_p$ is plotted against salt concentration s (moles of Li^+ per mole of PEO chains) on a (a) semi-log and (b) log-log plot. As explained in the text, s can also be interpreted as the effective chain length due to complexation with ions. The dotted line is the equation $D - D_p = Ks^{-1}$ where $K = -6.48$ cm^2/s . Error bars are omitted for clarity.

anion diffusion collapse onto a single curve of the form $(D - D_p) \propto s^{-1}$. The functional dependence is similar to that introduced by Shi and Vincent,²⁰ however, this new scaling theory takes into account both salt concentration and molecular weight effects on both ions. At low molecular weights and salt concentrations, transport of ions is strongly coupled to the relaxation modes of the PEO chains, which have an M^{-1} dependence based on the Rouse model.³⁵ At high molecular weights and high concentrations, chain diffusion slows down and transport is dominated by ion hopping facilitated by segmental motion.

Figure 7 indicates that the crossover between the two regimes of transport—decreasing D_+ and D_- with increasing s and the diffusivity plateau—is demarcated by a constant value of s , not M as proposed by Shi and Vincent.²⁰ The exact value of s at the crossover is not well-defined; eq 5 indicates that the diffusivity plateau is only reached asymptotically as s approaches infinity. From a practical point of view, however, we may assume that systems with $|D - D_p|$ smaller than 10^{-8} cm²/s are sufficiently close to the plateau. Figure 7b indicates that the crossover value of s , $s_c \approx 10$ for this cutoff. We propose that the importance of s to the crossover stems from the high probability that a lithium ion will coordinate with two PEO chains.^{28,36} We assume that this probability is independent of chain length. If the lifetime of this coordination is significant, then the “effective” chain length is increased and chain motion slows down. Transition to the diffusive plateau regime in electrolytes comprised of long chains thus requires low salt concentrations, while electrolytes comprised of short chains require higher salt concentrations. In other words, the crossover location is governed by the product $N \times r$, which is, by definition, s .

CONCLUSIONS

Individual self-diffusion coefficients of Li⁺ and TFSI⁻ ions, D_+ and D_- , were measured as a function of M and salt concentration. We found agreement between conductivities calculated from the measured D_+ and D_- values based on the Nernst–Einstein equation and experimental measurements of σ in both dilute and concentrated solutions, indicating that the salt is fully dissociated in these PEO/LiTFSI mixtures. This enabled the determination of the molecular weight dependence of the cation transference number in both concentration regimes. We introduce an important parameter s , the number of lithium ions per polymer chain. The dependences of D_+ and D_- on s allow us to account for salt concentration and chain length effects on the diffusion coefficients. Ion diffusion coefficients D_+ and D_- in both dilute and concentrated PEO/LiTFSI decrease at low s , and plateau above $s = 10$. We present a master curve that describes the dependence of both D_+ and D_- on salt concentration and chain length. The high molecular weight plateau seen in ionic conductivity measurements is due to the plateau of D_- ; the plateau of D_+ plays a minor role. In the high molecular weight limit, $D_{p,-}$ is significantly larger than $D_{p,+}$ indicating that TFSI⁻ ions are not affected by the slowly relaxing segments that impede the motion of Li⁺ ions. The scaling phenomena introduced in this work is not captured by prevailing theories^{20,25} and may be representative of all polymer electrolytes that selectively solvate one of the ions.

ASSOCIATED CONTENT

Supporting Information

The Supporting Information is available free of charge on the ACS Publications website at DOI: 10.1021/acs.macromol.5b01724.

Sample 1D spectra, Stejskal–Tanner plots, and a plot of D vs. M at all r . (PDF)

AUTHOR INFORMATION

Corresponding Author

*(N.P.B.) E-mail: nbalsara@berkeley.edu.

Author Contributions

The manuscript was written through contributions of all authors. All authors have given approval to the final version of the manuscript.

Notes

The authors declare no competing financial interest.

ACKNOWLEDGMENTS

This work was supported by the Division of Chemistry, National Science Foundation under grant NSF-CHE-1333736 in the Designing Materials to Revolutionize and Engineer our Future Program. We thank John Newman for educational discussions and Chris Canlas for help with NMR instrument and facilities support.

ABBREVIATIONS

Li ⁺	lithium
TFSI ⁻	bis(trifluoromethanesulfonyl)imide
PEO	poly(ethylene oxide)
r	molar salt concentration
M	molecular weight of polymer
D_{Li}	diffusivity of Li ⁺ containing species
D_{TFSI}	diffusivity of TFSI ⁻ containing species
σ	ionic conductivity
D_+	cation diffusivity
D_-	anion diffusivity
t_+	cation transference number
s	moles of Li ions per mole of polymer chains or effective chain length
N	number of monomers per chain
$D_{p,-}$	anion diffusivity at plateau
$D_{p,+}$	cation diffusivity at plateau
l_B	Bjerrum length
s_c	crossover value of s

REFERENCES

- Hallinan, D. T., Jr.; Balsara, N. P. *Annu. Rev. Mater. Res.* **2013**, *43* (1), 503–525.
- MacCallum, J. R.; Vincent, C. A. *Polymer Electrolyte Reviews*; Springer: Berlin, 1987; Vol. 1.
- Fenton, D. E.; Parker, J. M.; Wright, P. V. *Polymer* **1973**, *14* (11), 589.
- Lascaud, S.; Perrier, M.; Vallee, a; Besner, S.; Prud'homme, J.; Armand, M. *Macromolecules* **1994**, *27* (25), 7469–7477.
- Newman, J.; Thomas-Alyea, K. *Electrochemical Systems*; Wiley: New York, 2004.
- Newman, J.; Chapman, T. W. *AIChE J.* **1973**, *19* (2), 343–348.
- Ma, Y.; Doyle, M.; Fuller, T. F.; Doeff, M. M.; De Jonghe, L. C.; Newman, J. J. *Electrochem. Soc.* **1995**, *142* (6), 1859–1868.
- Doyle, M.; Newman, J. J. *Electrochem. Soc.* **1995**, *142* (10), 3465–3468.

- (9) Bhattacharja, S.; Smoot, S. W.; Whitmore, D. H. *Solid State Ionics* **1986**, *18*, 306–314.
- (10) Gorecki, W.; Jeannin, M.; Belorizky, E.; Roux, C.; Armand, M. *J. Phys.: Condens. Matter* **1995**, *7* (34), 6823–6832.
- (11) Gorecki, W.; Roux, C.; Clémancey, M.; Armand, M.; Belorizky, E. *ChemPhysChem* **2002**, *3* (7), 620–625.
- (12) Donoso, J. P.; Bonagamba, T. J.; Panepucci, H. C.; Oliveira, L. N.; Gorecki, W.; Berthier, C.; Armand, M. *J. Chem. Phys.* **1993**, *98* (12), 10026–10036.
- (13) Hou, J.; Zhang, Z.; Madsen, L. a. *J. Phys. Chem. B* **2011**, *115* (16), 4576–4582.
- (14) Green, P. F.; Kramer, E. J. *Macromolecules* **1986**, *19* (4), 1108–1114.
- (15) De Gennes, P. G. *J. Chem. Phys.* **1971**, *55* (2), 572–579.
- (16) Vrentas, J. S.; Duda, J. L. *Macromolecules* **1976**, *9* (5), 785–790.
- (17) Won, J.; Onyenemezu, C.; Miller, W. G.; Lodge, T. P. *Macromolecules* **1994**, *27* (25), 7389–7396.
- (18) Ehlich, D.; Sillescu, H. *Macromolecules* **1990**, *23* (6), 1600–1610.
- (19) Park, H. S.; Chang, T.; Lee, S. H. *J. Chem. Phys.* **2000**, *113* (13), 5502–5510.
- (20) Shi, J.; Vincent, C. *Solid State Ionics* **1993**, *60* (1), 11–17.
- (21) Teran, A. A.; Tang, M. H.; Mullin, S. A.; Balsara, N. P. *Solid State Ionics* **2011**, *203* (1), 18–21.
- (22) Devaux, D.; Bouchet, R.; Glé, D.; Denoyel, R. *Solid State Ionics* **2012**, *227*, 119–127.
- (23) Hayamizu, K.; Akiba, E.; Bando, T.; Aihara, Y. *J. Chem. Phys.* **2002**, *117* (12), 5929–5939.
- (24) Diddens, D.; Heuer, A.; Borodin, O. *Macromolecules* **2010**, *43* (4), 2028–2036.
- (25) Chattoraj, J.; Knappe, M.; Heuer, A. *J. Phys. Chem. B* **2015**, *119* (22), 6786–6791.
- (26) Borodin, O.; Smith, G. D. *J. Solution Chem.* **2007**, *36* (6), 803–813.
- (27) Wu, D. H.; Chen, A. D.; Johnson, C. S. *J. Magn. Reson., Ser. A* **1995**, *115* (2), 260–264.
- (28) Borodin, O.; Smith, G. D. *Macromolecules* **2006**, *39* (4), 1620–1629.
- (29) Chan, L. L.; Smid, J. *J. Am. Chem. Soc.* **1967**, *89*, 4547–4549.
- (30) Mao, G.; Saboungi, M. L.; Price, D. L.; Armand, M. B.; Howells, W. S. *Phys. Rev. Lett.* **2000**, *84* (24), 5536–5539.
- (31) Ratner, M. a.; Shriver, D. F. *Chem. Rev.* **1988**, *88* (1), 109–124.
- (32) Borodin, O.; Smith, G. D. *Macromolecules* **2000**, *33*, 2273–2283.
- (33) Singh, M.; Odusanya, O.; Wilmes, G. M.; Eitouni, H. B.; Gomez, E. D.; Patel, a J.; Chen, V. L.; Park, M. J.; Fragouli, P.; Iatrou, H.; Hadjichristidis, N.; Cookson, D.; Balsara, N. P. *Macromolecules* **2007**, *40* (13), 4578–4585.
- (34) Orädd, G.; Edman, L.; Ferry, A. *Solid State Ionics* **2002**, *152*, 131–136.
- (35) Rouse, P. E. *J. Chem. Phys.* **1953**, *21* (7), 1272–1280.
- (36) Webb, M. a.; Jung, Y.; Pesko, D. M.; Savoie, B. M.; Yamamoto, U.; Coates, G. W.; Balsara, N. P.; Wang, Z.-G.; Miller, T. F. *ACS Cent. Sci.* **2015**, *1*, 198–205.